10

Optical characteristics of boron-doped silicon wafers after rapid thermal annealing

© N.I. Staskov[1], A.A. Sergeychik[2], A.B. Sotsky[1], A.N. Pyatlitsky[2], V.A. Pilipenko[2], L.I. Sotskaya[3], D.V. Ponkratov[1], E.A. Chudakov[1], A.V. Shilov[1]

[1] Mogilev State A.A. Kuleshov University,
Mogilev, Belarus
[2] Central Office„Central Office“ Scientific and Technical Center, JSC„INTEGRAL“,
Minsk, Belarus
[3] Belarusian Russian University,
Mogilev, Belarus

e-mail: ni_staskov@mail.ru

Received September 04, 2024
Revised May 07, 2025
Accepted June 05, 2025

Optical properties of boron-doped silicon wafers KDB-12 with one matte surface subjected to rapid thermal annealing are investigated by spectral ellipsometry. The influence of the known surface oxide layer is excluded in the algorithm for calculating the permittivity of the semiconductor substrate. The band gap width and Urbach energy are calculated. The spectra of the real and imaginary parts of the permittivity are shifted relative to the corresponding spectra of c-Si to the short-wave region. The band of the imaginary part of the permittivity in the region of the second singularity point consists of several bands.

Keywords: permittivity spectra, refractive and absorption indices, band gap, Urbach energy, boron-doped silicon.

DOI: 10.61011/EOS.2025.08.62025.7045-25

Introduction

KDB-12 wafers (silicon doped with boron,*p*-semiconductor) are used at JSC „INTEGRAL“ (Minsk, Republic of Belarus) as substrates for depositing planar structures and are the main component of many electronic and optoelectronic devices. Modeling and manufacturing of such structures with ultrathin layers require knowledge of the optical characteristics of the wafers: band gap width, dielectric permittivity spectra, refractive and absorption indices. The manufacturing technology of KDB-12 wafers does not exclude the appearance of an SiO_2 layer on the working surface, whose parameters affect the determined optical characteristics. Accordingly, great attention is paid to the development of optical methods for monitoring the process of wafer surface preparation before forming planar structures. An important step in this preparation is the passivation of the semiconductor surface, since in the air environment oxide films naturally form on the surfaces of most materials. One possible way to improve the surface properties of KDB is rapid thermal processing (RTP) by optical pulses of a duration of seconds. RTP technology is promising for creating ultrathin layers of underlying gate dielectrics [1].

Numerous optical characteristics [2,3], are used to interpret the physical properties of semiconductors, which are determined by spectrophotometry and ellipsometry methods — methods of electrodynamic models. Since the number of such models is not limited, optical characteristics, for example of c-Si, may not coincide [4,5]. The main characteristic of a semiconductor is the dielectric permittivity

$$\varepsilon(\lambda) = \varepsilon_1(\lambda) - i\varepsilon_2(\lambda) = [n(\lambda) - ik(\lambda)]^2, \qquad (1)$$

which in Maxwell's material equations for nonmagnetic media ($\mu = 1$) determines the equations of applied optical methods. Moreover, the changes in optical properties of silicon structures are conventionally interpreted by changes in $\varepsilon_1(\lambda)$ and $\varepsilon_2(\lambda)$ in the region of Van Hove singularity points ($\lambda_1 = 291.8$ nm, $E_1 = 4.25$ eV), $\lambda_2 = 361.5$ nm, $E_2 = 3.43$ eV [6–9]. Besides $\varepsilon(\lambda)$ the spectra of refractive indices $n(\lambda)$ and absorption $k(\lambda)$ indices that enter equation (1), as well as important semiconductor characteristics in band theory — band gap width E_g and Urbach energy E_u — are of interest. Their values are determined from the absorption coefficient

$$\alpha(\lambda) = \frac{4\pi k(\lambda)}{\lambda} \qquad (2)$$

based on Tauc extrapolation [10] or extrapolation of an empirical dependence $\ln[\alpha(E)]$ by means of the function [11]

$$f(E) = \ln\{\alpha(1240/E_g)\exp[(E - E_g)/E_u]\}, \qquad (3)$$

where $E = 1240\lambda^{-1}$ is the photon energy in eV (λ in nm). The value E_u characterizes the degree of imperfection of the semiconductor's crystal structure. Note that *c*-Si has a band gap width of 1.10 eV [12] to 1.16 eV [13] for indirect interband transitions and 3.4 eV [12] to 4.19 eV [13] for direct interband transitions.

Studies [14–17] by various physical methods have established that the thickness of the surface SiO_2 layer on KDB-12 wafers after physicochemical treatment is ~ 1.75 nm, and after RTP is ~ 1 nm. The influence of ultrathin surfaceSiO_2, layers, which can cover the surfaces of *c*-Si-wafers, on the ellipsometric angles $\Delta(\lambda)$, $\psi(\lambda)$ and on the optical characteristics has been thoroughly investigated [6–8]. It was established that spectral features in the region of singularity points of *c*-Si weaken with increasing layer thickness. Since when determining the optical constants of substrates, such layers can be taken into account but it is difficult to exclude their influence, in practice a simplified electrodynamic model is sometimes used, in which the substrate is considered homogeneous, and its$\varepsilon(\lambda)$ is called the pseudo-dielectric function $\langle\varepsilon(\lambda)\rangle$. In this particular case, there exists an analytical determination of function $\langle\varepsilon(\lambda)\rangle$. Changes observed [14–17] by spectral ellipsometry in $\langle k(\lambda)\rangle$ and $\langle n(\lambda)\rangle$ in the UV region containing Van Hove singularity points allowed considering that RTP leads to increased structural perfection of the wafer surface layer as a result of solid-phase recrystallization. Reduction of the SiO_2 layer thickness to less than 3 nm is accompanied by the disappearance of the crystalline silicon structure and the appearance of an amorphous phase. At the same time, these changes occur due to crystallization of disturbed silicon near the Si-SiO_2, interface, as well as due to annealing of radiation defects formed in the SiO_2 layer. At a temperature near 950° the process of nanocrystal formation of Si in the dielectric layer begins.

The problem of experimental determination of substrate parameters in the presence of an ultrathin surface layer with previously unknown characteristics remains unsolved. This explains the existence of several alternative approaches to its investigation. These include: *i*) the model of a plane-parallel layer of effective medium [6–9]; *ii*) the Fermi model to represent the change of dielectric permittivity by layer thickness [19]; *iii*) the integral layer model [20]; *iv*) the polarized dipole layer model [21].

The ambiguity of the inverse optical problem solution for determining parameters of structures with surface layers also occurs in coherent multi-angle ellipsometry. When determining the thickness and refractive index of nanoscale films deposited on substrates with unknown thin transition layers, both real and numerical experiments with monochromatic ellipsometry (LEF3M, $\lambda = 632.8$ nm), show the feasibility of replacing the structure substrate [22] – transition layer by a substrate with $\langle n\rangle$ and $\langle k\rangle$. The work [23] presents dependencies of $\Delta(\theta)$ and $\psi(\theta)$ measured on LEF3M for silicon wafers of orientation $\langle 100\rangle$ (hole conductivity, $\rho = 1.5\Omega$S). When determining refractive index and thickness of the surface layer, it was assumed that the substrate has $n = 3.865$ and $k = 0.018$ or $n = 3.85$ and $k = 0.023$. It was found that calculated parameters for different substrates differ and depend on the angle of incidence. Calculations of five parameters of the reflecting structure showed that for a thermally grown layer $d = 8.6$ nm, $n = 1.46$, $k = 0.00014$, and substrate

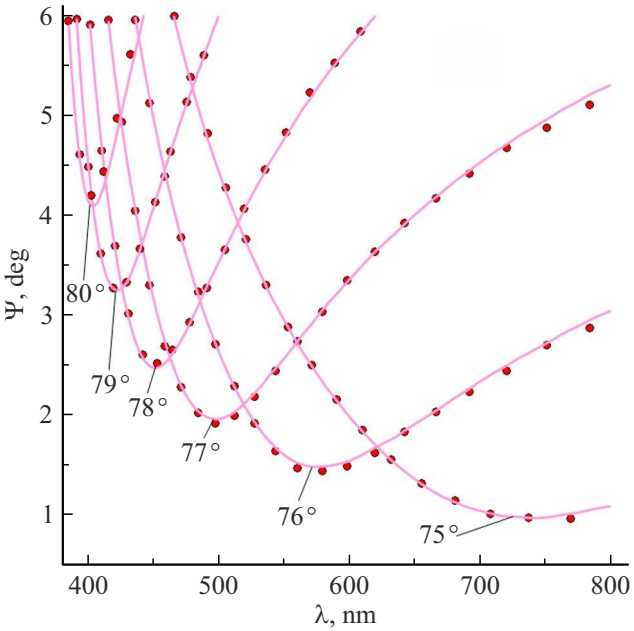

Figure 1. Measured (points) and calculated (lines) spectra of KDB-12 wafer.

characteristics in this case are $n = 3.81$, $k = 0.021$. In work [21] based on angular dependencies of$\Delta(\theta)$ and $\psi(\theta)$ measured on LEF3M, the following were obtained for the KDB-12 wafer $n = 3.83$, $k = 0.0001$, and for thermally grown SiO_2 layers of thickness 10 nm and 933 nm, $n = 1.46$ and $k = 0.0001$.

In [24] for *c*-Si ($\lambda = 546.1$ nm, $n = 4.05$, $k = 0.028$) dependencies of $\Delta(\theta)$, $\psi(\theta)$ and an angle of incidence $\theta = 76.13°$ are presented, for which $\Delta = 90°$, and ψ reaches a minimum value ($\psi_{\min}$). According to Brewster's law,

$$n = \tan(\theta) \tag{4}$$

is found to be $n = 4.05$. The spectral ellipsometry calculations of quartz glasses based on data by equation (4) were carried out in [25]. Possibly, Brewster spectral ellipsometry can be used as an independent method to assess the refractive index spectrum of semiconductors.

This communication develops a method to exclude the influence of the surface oxide layer located on KDB-12 wafers after RTP on the optical characteristics determined by ellipsometry methods. This made it possible to compare the main optical characteristics of pure and boron-doped silicon.

Methodology and experimental technique

Samples used were KDB-12 wafers ($N = 10^{15}$ cm^{-3}, $\rho = 12\Omega$ S) of orientation $\langle 100\rangle$ with a diameter of 100 mm, obtained by the Czochralski method. One surface of the wafers was subjected to mechanical processing and etched for (3 ± 1) min minutes in hydrofluoric acid solution. Then rapid thermal processing was

carried out by irradiating the non-working (matte) side of the wafer with a light pulse for 7 s in an Ar atmosphere at annealing temperature $(1025 \pm 1)^\circ$C. As a result of such sample preparation, the informativeness of optical methods is provided by the near-surface wafer layer with thickness on the order of the light penetration depth. When solving inverse ellipsometry problems for c-Si-substrates with an SiO_2 layer up to 2 nm thick using Deltapsi2 software installed on a Horiba UVISEL 2 ellipsometer, the discrepancy χ^2 between measured and calculated spectra $\Delta(\lambda)$, $\psi(\lambda)$ should not exceed 0.2.

The spectra $\Delta(\lambda)$ and $\psi(\lambda)$ of KDB-12 wafers subjected to rapid thermal annealing (RTP) were measured at room temperature using a Horiba UVISEL 2 ellipsometer at angles of incidence (θ) 70° (200 nm$\leq \lambda \leq$ 2000 nm), 73°–80°, (300 nm$\leq \lambda \leq$ 800 nm) and on LEF3M at incidence angles from 72°to 78° ($\Delta\theta = 2^\circ$). The reflection coefficients of s- and p-polarized lightR_s, R_p) of these wafers were measured on a PHOTON RT spectrophotometer (EssentOptics, Belarus) at incidence angles 30° and 60° (200 nm$\leq \lambda \leq$ 700 nm). The choice of incidence angles and spectral ranges for ellipsometry measurements was based on the recommendations of the DeltaPsi2 software.

Results and Discussion

We apply equation (4) to estimate the refractive indices of KDB-12 wafers. On the spectra of ellipsometric angles $\psi(\lambda)$measured at θ from 75° to 80°Brewster intervals are clearly identified (Fig. 1). Within these intervals, wavelengths can be determined at which the angle of incidence equals the pseudo-Brewster angle ($\psi = \psi_{\min}$). As θ increases, wavelengths corresponding to the main and pseudo-Brewster angles move into the ultraviolet (UV) region. Moreover, the difference between these wavelengths increases due to the increase in the semiconductor's absorption coefficient.

Table 1 lists the incidence angles, wavelengths corresponding to $\psi_{\min}$ and Brewster refractive indices n_{Br} for the KDB-12 wafer, calculated using equation (4). Optical characteristics at the wavelength 632.8 nm were numerically determined from ellipsometric angles measured on the LEF3M.

Assuming (problem A) that a plane-parallel SiO_2, $n(\lambda)$ layer with refractive index given analytically [26] lies on a homogeneous substrate. Its complex dielectric permittivity $\varepsilon(\lambda)$ is modeled by a 4-oscillator amorphous materials [27] model with unknown parameters ε_∞, E_g, A_ξ, B_ξ, C_ξ, where $\xi \in 1 \div 4$. These fitting parameters are selected by DeltaPsi2 software to calculate the layer thickness, material composition, and spectra $k(\lambda)$, $n(\lambda)$ of the substrate. For all unknown parameters (Table 2, row A) measured spectra $\Delta(\lambda)$ and $\psi(\lambda)$ at incidence angles 73° – 80°were used. Initial approximations for ε_∞, E_g, A_ξ, B_ξ, C_ξ of the 4-oscillator model were taken from DeltaPsi2 recommendations for c-Si. Table 1 shows refractive and absorption indices of the KDB-12 substrate for this ellipsometric inverse problem. Consider the calculation results (Table 2, row A): i) $\chi^2 > 0.2$; ii) the fitted parameter $E_g = 2.73$ eV indicates that boron doping shifts the absorption edge into the visible region, and for $\lambda > 454.2$ nm the KDB-12 wafer should be transparent; iii) theSiO_2 layer thickness is 2.4 times larger than values determined by non-optical methods in [14–17]. These factors indicate the need for a more complex electrodynamic model of the KDB-12 substrate.

Assuming (problem B) that on a substrate, whose dielectric function $\varepsilon(\lambda)$ is modeled by a 4-oscillator amorphous material model, there are five Bruggeman layers. The parameters of the layers, starting from the one on the substrate, have indices $j \in 1 \div 5$. Two-component effective Bruggeman layers include c-Si (f%) and KDB-12 ($(100 - f)$%), while the surface layer ($j = 5$) contains SiO_2 (f%) and c-Si $(100 - f)$%) or SiO_2 (f%) and amorphous silicon (α-Si, $(100 - f)$%). Thicknesses and material compositions of these layers were determined using DeltaPsi2 software. This electrodynamic substrate model is partly based on conclusions of [18]. Results of problem B are given in Table 2. Analysis shows: i) the KDB-12 wafers after RTP have a surface SiO_2, layer of thickness ($d_s = 1.1$ nm) matching values from [14–17]; ii) beneath this SiO_2 layer there is a heterogeneous layer 71.4 nm thick in which c-Si concentration increases from 24.2% toward 100% near the working surface (with corresponding decrease in KDB-12 content); iii) refractive indices calculated for this model are close to n_{Br} (Table 1); iv) the fitted parameter $E_g = 2.92$ eV confirms that boron doping shifts the absorption edge into the visible and that KDB-12 is transparent at $\lambda > 424.7$ nm.

An attempt was made (problem C) to exclude the plane-parallel SiO_2 layer of known thickness ($d = 1.1$ nm) and known refractive index [26] in the algorithm calculating spectra $n(\lambda)$ and $k(\lambda)$ of the KDB-12 substrate (Table 1), whose complex dielectric permittivity $\varepsilon(\lambda)$ is found without any dispersion model. In the algorithm, ε is the root of the equation

$$f(\varepsilon) = \tan\psi \exp(i\Delta), \tag{5}$$

where ψ and Δ are experimental polarization angles,

$$f(\varepsilon) = \frac{r_p}{r_s} = \frac{(\psi_p i n_a \cos\theta - \psi'_p n_a^2)(\psi_s i n_a \cos\theta + \psi'_s)}{(\psi_p i n_a \cos\theta + \psi'_p n_a^2)(\psi_s i n_a \cos\theta - \psi'_s)},$$

r_p and r_s are amplitude reflection coefficients of p- and s-polarized waves from the layer SiO_2 KDB-12 substrate structure,

$$\psi_p = \left(z^2 + n_a^2 \sin^2\theta\right)\cos(\sigma k_0 d) + iz\varepsilon_f \sigma^{-1} \sin(\sigma k_0 d),$$

$$\psi'_p = iz\cos(\sigma k_0 d) - (z^2 + n_a^2 \sin^2\theta)\sigma\varepsilon_f^{-1}\sin(\sigma k_0 d),$$

$$\psi_s = \cos(\sigma k_0 d) + iz\sigma^{-1}\sin(\sigma k_0 d),$$

$$\psi'_s = iz\cos(\sigma k_0 d) - \sin(\sigma k_0 d),$$

Table 1. Optical characteristics of KDB-12 wafers

θ°	λ, nm	n_{Br}	Problem *A*		Problem *B*		Problem *C*	
			n	*k*	*n*	*k*	*n*	*k*
80	403.8	5.671	5.475	0.110	5.567	0.042	5.392	0.316
79	422.4	5.147	5.036	0.026	5.102	0.00005	4.998	0.209
78	457.7	4.705	4.561	0	4.599	0	4.551	0.120
77	497.9	4.332	4.266	0	4.291	0	4.276	0.080
76	573.9	4.011	3.975	0	3.992	0	3.982	0.048
–	632.8	3.853	3.848	0.028	3.865	0.028	3.852	0.033
75	742.4	3.732	3.705	0	3.727	0	3.711	0.023

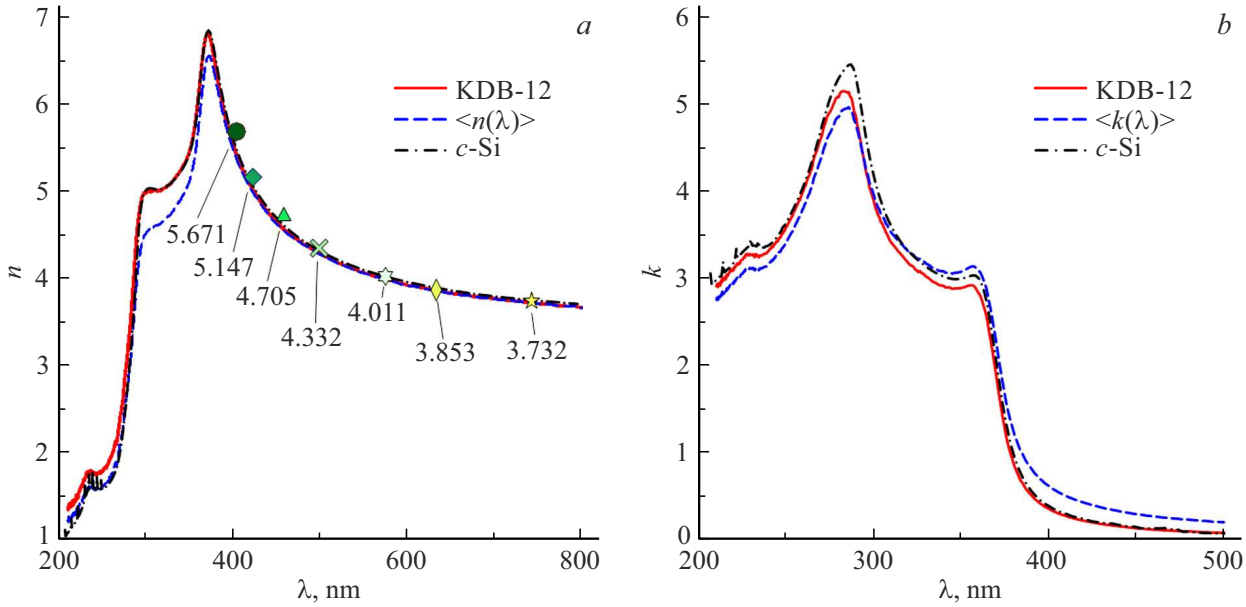

Figure 2. Optical characteristics of KDB-12 wafer and*c*Si.

$k_0 = 2\pi/\lambda$, $z = \sqrt{\varepsilon - n_a^2 \sin^2\theta}$, $\sigma = \sqrt{\varepsilon_f - n_a^2 \sin^2\theta}$, $n_a = 1.0003$ — refractive index of air. To avoid problems computing complex radicals, it is expedient to choose ε as the unknown quantity in equation (5) instead of z. Then equation (5) reduces to a cubic equation in z, which can be solved by the contour integration method [28]. $\varepsilon = z^2 + n_a^2 \sin^2\theta$ is found after calculating z. Spectra $\Delta(\lambda)$ and $\psi(\lambda)$, measured at $\theta = 70^\circ$. were used in calculations. Initial approximations for $\varepsilon_1(\lambda)$ and $\varepsilon_2(\lambda)$ were dielectric functions of *c*-Si. Table 2 confirms the known conclusion that the results of inverse optical problems depend on the chosen sample models. Figure 2 shows spectra $\langle n(\lambda)\rangle$, $n(\lambda)$ (*a*), and spectra $\langle k(\lambda)\rangle$, $k(\lambda)$ (*b*). Spectra of optical characteristics of *c*-Si on this figure are taken from [4].

In the visible region (380 nm $\leq \lambda \leq$ 800 nm) inequalities $n_{\mathrm{Br}} > n_{c\,\mathrm{Si}} > n_{\mathrm{KDB}} > \langle n\rangle$ and $\langle k\rangle > k_{\mathrm{KDB}} > k_{c\,\mathrm{Si}}$for refractive and absorption indices hold. The refractive indices n_{Br} are the maximum possible for KDB-12. The maxima of the spectra $\langle k(\lambda)\rangle$, $k_{c\mathrm{Si}}(\lambda)$ and $k_{\mathrm{KDB}}(\lambda)$ are shifted toward the short-wave region ($\Delta\lambda > \Delta\lambda_{\mathrm{KDB}} > \Delta\lambda_{c\mathrm{Si}}$) relative to the corresponding singularity points at 291.8 nm and 361.5 nm.

To determine the band gap width of the investigated semiconductor, the method proposed in [11] was used. The experimental dependence $\ln[\alpha_1(E)]$ Fig. 3) shows two linear regions, whose linear interpolation by lines (3) in the interval 0.62 eV $\leq E \leq$ 1.88 eV gives $E_{g1} = 1.04$ eV, $E_{u1} = 0.32$ eV and in the interval 1.88 eV $\leq E \leq$ 2.8 eV the interpolation yields $E_{g2} = 1.98$ eV and $E_{u2} = 0.51$ eV.

Similar calculations for *c*-Si are shown in Fig. 3. To determine $\ln[\alpha_2(E)]$ data from $k(\lambda)$ [4] were used. In this case, there is one linear region whose linear interpolation by line (3) yields the characteristic $E_g = 1.14$ eV of crystalline silicon. On the curve, two linear regions can also be distinguished, whose linear interpolation by lines (3) in the range 0.62 $\leq E \leq$ 1.39 eV gives $\langle E_{g1}\rangle = 1.08$ eV and $\langle E_{u1}\rangle = 0.43$ eV, and in the range 1.39 eV$\leq E \leq$ 2.8 eV we have $\langle E_{g2}\rangle = 1.81$ eV and $\langle E_{u2}\rangle = 0.63$ eV. Close values of E_{g1} and $\langle E_{g1}\rangle$ for KDB-12 wafers are due to the small thickness of the near-surface SiO_2 layer.

Table 2. Results of the inverse problems A and B of spectral ellipsometry

Problem	E_g, eV	ε_∞	A_ξ, eV	B_ξ, eV	C_ξ, eV^2	f, %	d_j, nm
A	2.73	6.366	0.068 0.165 0.546 -0.582	6.863 7.329 8.665 7.673	11.793 13.520 18.525 17.263	100	$d_1 = 2.42$
B	2.92	8.047	0.122 0.545 0.027 0.197	6.871 7.190 11.578 8.910	11.819 13.092 33.806 20.010	$f_1 = 24.2$ $f_2 = 61.9$ $f_3 = 84.0$ $f_4 = 100$ $f_5 = 100$	$d_1 = 22.2$ $d_2 = 25.2$ $d_3 = 23.6$ $d_4 = 0.4$ $d_5 = 1.1$

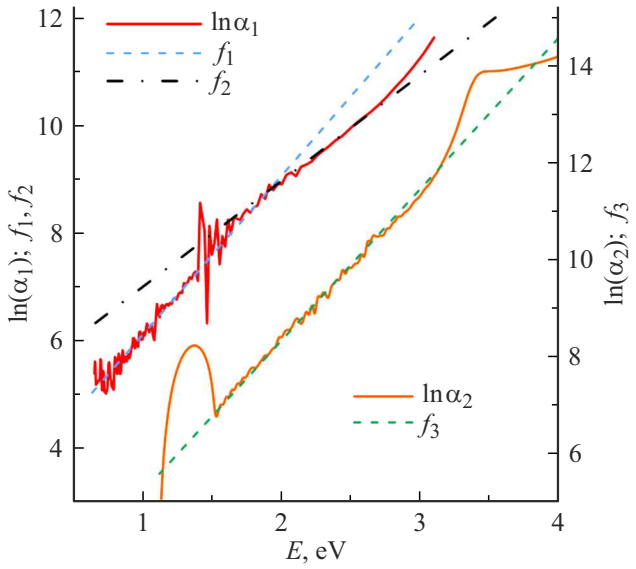

Figure 3. Calculation of the band gap width of KDB-12 and c-Si.

In [29] Tauc graphs are presented for determining the optical band gap width of Si@O@Al nanocomposite films on quartz substrates. The graphs also show two regions: a short linear region near$E < 2.0$ eV attributed to absorption contribution of nanocrystalline silicon($E_g = 1.15$ eV), and a longer almost linear region ($E > 2.0$ eV) due to the nanocomposite absorption contribution.

The presented data (Fig. 3) show a decrease in the silicon band gap width upon boron doping for indirect and direct transitions. This decrease is due to the location of the impurity acceptor levels in the forbidden gap near the valence band edge.

The defined criteria for verifying solutions of inverse ellipsometry problems A–C are: i) the smallest discrepancy value χ^2 equal to 0.07, between measured and calculated reflection coefficients R_s, R_p at two incidence angles is achieved with an SiO_2 layer thickness of 1.1 nm using spectra $k(\lambda)$, $n(\lambda)$ of the KDB-12 wafer from solution C; ii) the refractive indices of the KDB-12 wafer at $\lambda = 632.8$ nm (Table 1), determined by spectral (problem C) and monochromatic ellipsometry methods, almost coincide; iii) width of bandgaps (Fig. 3) KDB-12 and c-Si (% was used to determine them)$k(\lambda)$ from problem C); iii) satisfactory correlation of values for c-Si $k(\lambda)$, $n(\lambda)$ for $\lambda = 632.8$ nm (Table 1) agree well with data from [23].

In [30] photoacoustic spectra for KDB with boron content ($N = 4. \cdot 10^{18}$ cm^{-3}) determined $E_g = 1.06$ eV. With increasing boron impurity concentration $N = 4 \cdot 10^{20}$ cm^{-3} a red shift of $\langle\varepsilon_1(\lambda)\rangle$ and $\langle\varepsilon_2(\lambda)\rangle$ toward longer wavelengths and an increase in lifetime at two singularities E_1 and E_2were observed.

Figure 4 shows dielectric permittivity spectra of the KDB-12 wafer and c-Si. The first Van Hove singularity point ($\lambda_1 = 291.8$ nm) for c-Si is characterized by $\varepsilon_1 = -4.24$for KDB-12 by $\varepsilon_1 = 1.08$ and $\langle\varepsilon_1\rangle = -3.36$. The second Van Hove singularity point ($\lambda_2 = 361.5$ nm) is characterized for c-Si, $\varepsilon_1 = 29.69$ and for KDB-12 by $\varepsilon_1 = 31.17$ and $\langle\varepsilon_1\rangle = 25.19$. The wavelengths characterizing maxima ε_2 of the two Van Hove singularity points for c-Si and KDB-12 do not coincide. Near the first singularity point for c-Si $\varepsilon_2(291.8) = 46.82$ and for KDB-12 $\varepsilon_2(290.2) = 44.16$ and $\langle\varepsilon_2(291.1)\rangle = 38.58$ are observed. Maxima of the $\varepsilon_2(\lambda)$ function for KDB-12 relative to maxima of c-Si are shifted toward shorter wavelengths or higher energies (blue shift). Near the second point for c-Si $\varepsilon_2(361.5) = 36.43$ and for KDB-12 $\varepsilon_2(360.3) = 34.47$ and $\langle\varepsilon_2(362.2)\rangle = 35.64$ are observed. The maximum of function $\varepsilon_2(\lambda_2)$ for KDB-12 relative to the corresponding maximum for$c$-Si is shifted toward shorter wavelengths or higher energies (blue shift). However, the maximum of function $\langle\varepsilon_2(\lambda_2)\rangle$ for KDB-12 relative to the corresponding maximum $\varepsilon_2(\lambda_2)$ c-Si is shifted toward longer wavelengths or lower energies (red shift), similarly to [31].

Conclusion

By excluding a known plane-parallel surface layer in the algorithm calculating the main optical spectra of the semiconductor substrate using spectral ellipsometry without any dispersion model, the following functions and characteristic parameters have been determined for KDB-12 wafers after RTP: $\varepsilon_1(\lambda)$ and $\varepsilon_2(\lambda)$; $n(\lambda)$ and

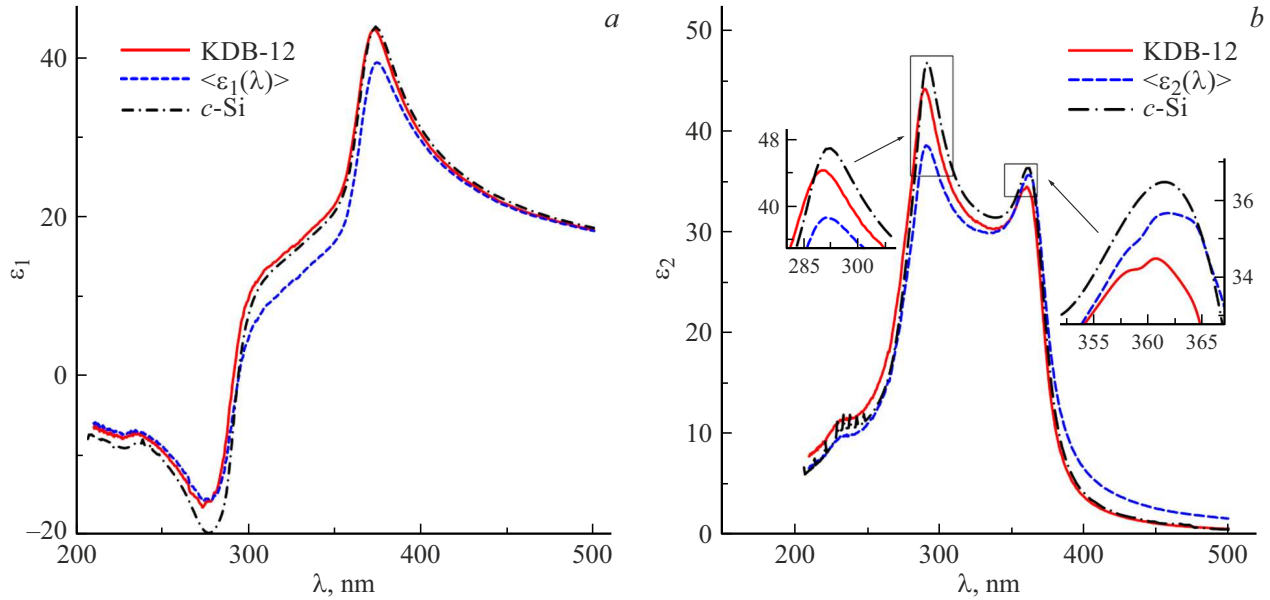

Figure 4. Dielectric permittivities of KDB-12 and *c*-Si.

$k(\lambda)$; band gap widths$E_g^{indir} = 1.04\,\text{eV}$ and $E_g^{dir} = 1.98\,\text{eV}$; Urbach energies $E_u^{indir} = 0.32\,\text{eV}$ and $E_u^{dir} = 0.51\,\text{eV}$. The technological process of producing KDB-12 wafers, which includes boron doping of silicon during crystal growth, physicochemical treatment, and rapid thermal annealing for surface passivation, leads to the formation under the SiO_2 layer of a thickness-nonuniform layer with uneven boron incorporation into the crystal lattice of *c*-Si. The main cause of nonuniformity is the rapid thermal annealing of KDB-12 wafers. Differences between KDB-12 and *c*-Si: i) in the visible range ($380\,\text{nm} \leq \lambda \leq 800\,\text{nm}$) refractive and absorption indices satisfy inequalities $n_{\text{Br}} > n_{c\text{Si}} > n_{\text{KDB}} > \langle n \rangle$ and $\langle k \rangle > k_{\text{KDB}} > k_{c\text{Si}}$; ii) maxima of the spectra $\langle k(\lambda) \rangle$, $k_{c\text{Si}}(\lambda)$ and $k_{\text{KDB}}(\lambda)$ are shifted towards the short-wave region ($\langle \Delta\lambda \rangle > \Delta\lambda_{\text{KDB}} > \Delta\lambda_{c\text{Si}}$) relative to Van Hove singularity points at 291.8 nm and 361.5 nm; iii) boron doping decreases the silicon band gap widths for indirect and direct transitions; iv) $\varepsilon_1(\lambda)$ and $\varepsilon_2(\lambda)$ spectra of KDB-12 are shifted relative to *c*-Si spectra toward short wavelengths; v) the function $\varepsilon_2(\lambda)$ near the second singularity point has a complex structure.

Brewster-angle spectral ellipsometry may be used for rapid estimation of refractive index dispersion of wafers in the visible spectral region.

Funding

This work was carried out within the State Scientific Research Program of the Republic of Belarus „1.15 Photonics and Electronics for Innovations“.

Conflict of interest

The authors declare no conflict of interest.

References

[1] A.M. Svetlichnyj, O.A. Ageev, D.A. Shlyahovoj. Tekhnologiya i konstruirovanie v elektronnoj apparature, **4**–**5**, 38 (2001). (in Russian)
[2] Yu.I. Ukhanov. *Opticheskie svoistva poluprovodnikov* (Nauka, M., 1977) (in Russian).
[3] H.S. Koval'chuk, A.A. Omel'chenko, V.A. Pilipenko, V.A. Soloduha, D.V. Shestovskij. BGUIR Reports, **4**, 103 (in Russian). (2021). DOI: 10.35596/1729-7648-2021-19-4-103-112
[4] E.D. Palik. *Handbook of Optical Constants of Solids* (Academic press, Orlando, 1985).
[5] Martin A. Green, Mark J. Keevers. Progress in Photovoltaics: Research and Applications, **3**, 189 (1995).
[6] H.G. Tompkins, E.A. Irene. *Handbook of Ellipsometry* (Inc. Springer, USA, 2005).
[7] H. Fujiwara. *Spectroscopic Ellipsometry: Principles and Applications* (John Wiley & Sons, Ltd, 2007).
[8] D.E. Aspnes, A.A. Studna. Phys. Rev. B, **27** (2), 985 (1983).
[9] G.E. Jellison. Thin Solid Films, **313**–**314**, 33 (1998).
[10] J. Tauc, R. Grigorovici, A. Vancu. Phys. Status Solidi B, **15**, 627 (1966).
[11] N.V. Gaponenko, N.I. Staskov, L.V. Sudnik, P.A. Vityaz, A.R. Luchanok, Yu.D. Karnilava, E.I. Lashkovskaya, M.V. Stepikhova, A.N. Yablonskiy, V.D. Zhivulko, A.V. Mudryi, I.L. Martynov, A.A. Chistyakov, N.I. Kargin, V.A. Labunov, Yu.V. Radyush, E.B. Chubenko, V.Yu. Timoshenko. Photonics, **10**(4), 359 (2023). DOI: 10.3390/photonics10040359
[12] J. Noffsinger, E. Kioupakis, C.G. Van de Walle, S.G. Louie, M.L. Cohen. Phys. Rev. Lett., **108**, 167402 (2012). DOI: 10.1103/PhysRevLett.108.167402
[13] K.W. Böer, U.W. Pohl. *Semiconductor* Physics (Springer. Library of Congress Control Number: 2017957993). DOI: 10.1007/978-3-319-69150-3

[14] V.A. Solodukha, U.A. Pilipenko, A.A. Omelchenko, D.V. Shestovski. Devices and Methods of Measurements, **13**(3), 199 (2022). DOI: 10.21122/2220-9506-2022-13-3-199-207
[15] V.A. Pilipenko, V.A. Soloduha, V.A. Gorushko, A.A. Omel'chenko. Dokl. Nats. akad. nauk Belarusi, **3** (347), 2018 (in Russian). DOI: 10.29235/1561-8323-2018-62-3-347-352
[16] V.M. Anishchik, V.A. Gorushko, V.A. Pilipenko, V.V. Ponaryadov, V.A. Soloduha, A.A. Omel'chenko. Zhurnal Belorusskogo gosudarstvennogo universiteta. Fizika, **3**, 81 (2021) (in Russian).
[17] V.A. Soloduha, A.I. Belous, G.G. Chigir'. Nauka i tekhnika. **15**(4), 329 (2016). DOI: 10.21122/2227-1031-2016-15-4-329-334
[18] V.A. Shvec, E.V. Spesivcev, S.V. Ryhlickij, N.N. Mihajlov. Rossiyskiye nanotekhnologii, **4** (3) (72), 2009 (in Russian).
[19] I.V. Ivashkevich, N.I. Stas'kov, A.B. Sotskij, L.I. Sotskaya, N.A. Krekoten', L.D. Bujko. Izvestiya GGU, **39** (6, ch. 2), 60 (2006). (in Russian)
[20] N.I. Stas'kov, I.V. Ivashkevich, A.B. Sotskij, L.I. Sotskaya. Problemy fiziki, matematiki i tekhniki, **1**(10), 26 (2012). (in Russian)
[21] N.I. Staskov, L.I. Sotskaya. J. Appl. Spectrosc., **84**(5), 764 (2017). DOI: 10.1007/s10812-017-0542-z
[22] D.I. Bilenko, V.P. Polyanskaya, M.A. Gec'man, D.A. Gorin, A.A. Neveshkin, A.M. Yashchenok. ZhTF, **75** (6), 69 (2005). (in Russian)
[23] B.M. Ayupov, V.A. Gritsenko, Hei Wong, C. W. Kimd. J. Electrochemical Society, **153**(12), F277 (2006).
[24] R. Azam, N. Bashara. *Ellipsometriya i polyarizovannyj svet* (Mir, M., 1981). (in Russian)
[25] N.I. Stas'kov, A.A. Muhammedmuradov, N.A.Krekoten', S.O. Parashkov. Zhurnal prikladnoy spektroskopii **87**, (1), 122 (2020) (in Russian).
[26] I.H. Malitson. J. Opt. Soc. Am., **55**(10), 1205 (1965).
[27] A.R. Forouhi, I. Bloomer. Phys. Rev. B, **38**(3), 1865 (1988).
[28] A.B. Sotskij. *Teoriya opticheskih volnovodnyh elementov* (UO MGU im. A.A. Kuleshova, Mogilev, 2011). (in Russian)
[29] A.S. Rudyj, A.B. Churilov, S.V. Kurbatov, A.A. Mironenko, V.V. Naumov, E.A. Kozlov. ZhTF, **93** (10), 1447 (2023) (in Russian). DOI: 10.61011/JTF.2023.10.56283.93-23
[30] J.C. de Souza, A.F. da Silva, H. Vargas. J. Physique, **IV**(4(C7)), C7-129 (1994).
[31] L. Vina, & M. Cardona. Phys. Rev. B, **29**(12), 6739 (1984).

Translated by J.Savelyeva